Predicting Tunnel Squeezing Using the SVM-BP Combination Model

Zhen HUANG (hzcslg@163.com)
Central South University https://orcid.org/0000-0003-2026-5893
Minxing Liao
Guangxi University
Haoliang Zhang
Guangxi University
Jiabing Zhang
Guangxi University
Shaokun Ma
Guangxi University
Qixuan Zhu
Guangxi University

Research Article

Keywords: tunnel squeezing, support vector machine, back-propagation, classification performance, machine learning

Posted Date: April 19th, 2021

DOI: https://doi.org/10.21203/rs.3.rs-379738/v1

Version of Record: A version of this preprint was published at Geotechnical and Geological Engineering on August 12th, 2021. See the published version at https://doi.org/10.1007/s10706-021-01970-1.

Predicting Tunnel Squeezing Using the SVM-BP Combination Model

Zhen Huang[1,2], Minxing Liao[1], Haoliang Zhang[1], Jiabing Zhang[1,2*], Shaokun Ma[1], Qixuan Zhu[1]

(1. College of Civil Engineering and Architecture, Guangxi University, Nanning, 530004, China； 2. Guangxi University Key Laboratory of Engineering Disaster Prevention and Structural Safety, Nanning, 530004, China)

Zhen Huang: hzcslg@163.com

Minxing Liao: liaominxing2348@163.com

Haoliang Zhang: zhl18818692636@163.com

Jiabing Zhang*: zhang_jb1@sohu.com

Shaokun Ma: mashaokun@sina.com

Qixuan Zhu: kylin_0702@163.com

Abstract: Rock squeezing has a large influence on tunnel construction safety; thus, when designing and constructing tunnels it is highly important to use a reliable method for predicting tunnel squeezing from incomplete data. In this study, a combination SVM-BP (support vector machine-back-propagation) model is proposed to classify the deformation caused by surrounding rock squeezing. We designed different characteristic parameters and three types of classifiers (an SVM model, a BP model, and the proposed SVM-BP model) for the tunnel-squeezing prediction experiments and analysed the accuracy of predictions by different models and the influences of characteristic parameters on the prediction results. In contrast to other prediction methods, the proposed SVM-BP model is verified to be reliable. The results show that four characteristics: tunnel diameter (D), tunnel buried depth (H), rock quality index (Q) and support stiffness (K) reflect the effect of rock squeezing sufficiently for classification. The SVM-BP model combines the advantages of both an SVM and a BP neural network. It possesses flexible nonlinear modelling ability and the ability to perform parallel processing of large-scale information. Therefore, the SVM-BP model achieves better classification performance than do the

SVM or BP models separately. Moreover, coupling D, H, and K has a significant impact on the predicted results of tunnel squeezing.

Keywords: tunnel squeezing; support vector machine; back-propagation; classification performance; machine learning

1 Introduction

Tunnel-surrounding rock squeezing is a deformation based on a space-time relationship that usually occurs in soft rock surrounding tunnels at large buried depths. Rock squeezing has a large impact on the tunnel construction safety (Wang, 2020). The negative consequences of tunnel squeezing have been reported repeatedly since it was first discovered during the construction of the Simplon Tunnel in Switzerland (Yassaghi and Salari-Rad, 2005). Tunnel squeezing usually causes construction delays, budget overruns, shield blockage and even possibly results in tunnel instability as well as casualties (Sun, et al. 2018). Therefore, when designing and constructing tunnels it is very important to adopt a reliable method for predicting rock squeezing surrounding the tunnel.

In view of the practical importance of this topic, many scholars have attempted to develop methods for predicting tunnel squeezing. These prior approaches include both theoretical analytical methods (Fritz, 2010) and numerical simulation methods (Debernardi and Barla, 2009; Gao, et al. 2015). The analytical solution of time-dependent (or creep) deformation or numerical solutions for the advanced time-dependent constitutive model requires strong theoretical calculation ability that often exceeds the ability of many design and construction technicians. Some empirical methods are also included; these are often based on abundant reliable data (e.g., indicators of rock mass) or ~~on the use of~~ geometric classifications (RMR or Q systems). For instance, the ratio between rock mass uniaxial strength, σ_{cm},

and lithostatic stress, $\sigma_0 = \gamma_r H$ was used to predict tunnel squeezing by (Jethwa and Singh, 1984) and (Hoek and Marinos, 2000) ; for example, (Hoek, 2001) proposed that it is possible to produce squeezing with the values of σ_{cm}/σ_0 <0.35 (as defined by normalized convergences of more than 1% in unsupported tunnels); (Singh et al. 1992) presented a well-known empirical correlation related to the Q-value of the rock mass to predict squeezing conditions, in which tunnels deeper than $H = 350Q^{1/3}$ (where H is in metres) could possibly present squeezing. Considering the practical difficulties in predicting the stress reduction factor (SRF) in the Q system, the above methods are still the main approaches for predicting tunnel squeezing in practice, and they play an important role. (For an in-depth review of these and other methods for empirical squeezing prediction; see Singh et al. 1997 and Jimenez and Recio 2011.)

Machine learning methods have attracted extensive attention from researchers and have been applied to many aspects of tunnel engineering prediction. Machine learning methods may be useful tools for predicting tunnel squeezing. At present, the main machine learning methods for predicting tunnel-surrounding rock squeezing include regression analysis (Jimenez and Recio, 2011; Ghasemi and Gholizadeh, 2018), neural networks (Zhou, et al. 2018), decision trees (Chen, et al. 2020), naive Bayes (Feng and Jimenez, 2015), and support vector machines (Sun, et al. 2018; Shafiei, et al. 2012). However, the prediction ability of combination models based on machine learning still needs further exploration.

Among many machine learning methods, SVMs have strong generalization abilities and flexible nonlinear modelling ability, applying to solving small sample, high dimensional and nonlinear problems. Nevertheless , the SVM classifier is a binary classifier that cannot provide the posterior probability for a given pattern and can lead to results with extremely poor accuracy (Shafiei, et al. 2012;

Mahdevari, et al. 2013). The BP neural network has the ability to perform parallel processing of large-scale information, nonlinear mapping ability, and self-adaptive and reasoning generalization ability. The output of the model can be changed by altering the weight and threshold value of the model. However, the structure of the BP neural network is complex and changeable, and the gradient descent method can cause the results to fall easily into a local minimum. Therefore, the BP neural network has limited ability to solve small-sample problems (Ding, et al. 2011; Jin, et al. 2000). Thus, it seems to be logical to try to combine the advantages of an SVM and a BP neural network to establish a new combination model that could improve the accuracy of prediction results.

The goals of this study are to develop a combined model of SVM and BP for large-scale tunnel-squeezing prediction and to verify the robustness of the combined model by comparing it with other machine learning methods. This paper mainly includes the selection process for prediction parameters and statistical analyses, the construction of a prediction model, the analysis of the prediction results, and a conclusion and discussion. During the selection of prediction parameters and statistical analyses, the basis for the selection of surrounding rock parameters is analysed, a database containing surrounding rock sample indexes is established. The data are pre-processed and analysed statistically. In the section on prediction model construction, this paper introduces three different classifiers: SVM, BP, and SVM-BP combination models. In the prediction results analysis, the surrounding rock squeezing is classified and predicted according to the surrounding rock index data. The accuracy of the three models is compared, and the prediction results of other methods reported in the literature are compared. The results show the robustness of the SVM-BP combination model. Finally, the accuracy of the three models under different combinations of surrounding rock indexes is analysed. The conclusion and discussion section concludes the study and discusses the applicability of

90 the three models for rock-squeezing prediction.

91 2. Selection of the prediction parameters and data analyses

92 2.1 Selection and source of parameters

93 The tunnel parameters and surrounding rock indexes reflect the basic characteristics of the tunnel and
94 surrounding rock, respectively and are the most reliable parameters for predicting tunnel squeezing.
95 Based on of a literature review, the previously published methods for predicting tunnel squeezing are
96 summarized, as shown in Table 1. We can clearly see that many scholars have mainly adopted features
97 such as the tunnel buried depth (*H*), rock quality index (*Q*), tunnel diameter (*D*), support stiffness (*K*),
98 and stress intensity ratio (*SSR*) as prediction parameters, but these prior studies seldom considered the
99 vertical in situ stress and surrounding rock classification index (*GC)* based on the BQ system. Some of
100 the above parameters are difficult to adopt as prediction parameters for various reasons, such as the
101 vertical in situ stress and *GC,* which are often difficult to obtain in the early stages of a project. The
102 SSR is often difficult to obtain from engineering; consequently, much of the existing literature omits
103 data regarding the SSR. Therefore, this study adopts four easy-to-obtain parameters (*H*, *Q*, *D*, and *K*) as
104 input variables to predict tunnel squeezing.

105 Table 1. Correlation summary of previously published large scale prediction methods

Sources of references	Prediction method	Indicators considered	Number of samples
Singh, et al. (1992)	$H \geq 350Q^{0.32}$	*H*, *Q*	39
Goel, et al. (1995）	$H^3 270N^{0.33}D^{-0.1}, N=(Q)_{SRF=1}$	*D*, *Q*, *N*	72
Jimenez and Recio (2011)	$H^3 424.4Q^{0.32}$	*H*, *Q*	62
Shafiei, et al. (2012)	SVM	*H*, *Q*	198
Dwivedi, et al. (2013)	$\varepsilon = \frac{D^{0.12}H^{0.81}}{10.5N^{0.27}K^{0.62}}$	σ_v , *Q*, *K*	63
Feng, et al. (2015)	Naive Bayes	*H*, *D*, *Q*, *K*, *SSR*	166
Sun, et al. (2018)	SVM	*H*, *D*, *Q*, *K*	117
Chen, et al. (2020)	Coupling decision tree classifier, Bayesian and Markov geological model	*H*, *D*, *K*, *SSR, GC*	154
Zhang, et al. (2020)	SVM, ANN, KNN, DT, LR, MLR, NB weighted combination classifier	*H*, *D*, *Q*, *K*, *SSR*	166

106 The sample cases collected in this paper are compiled were Sun et al. (2018) and Dwivedi et al. (2013).
107 These cases include 180 large-scale tunnel-squeezing historical cases from Austria, Nepal, India,
108 Bhutan and other countries. These case databases contain the adopted *H*, *Q*, *D* and *K* parameters. Based
109 on the preliminary statistics of 180 tunnel squeezing cases, four parameter ranges were obtained in
110 which *D* ranges from 1.25 m to 13 m, *H* from 52 m to 850 m, *Q* from 0.001 to 93.5, and *K* from 0 kPa
111 to 5324 kPa. These data are used as model input variables. The output variable indicates the
112 prediction—whether the surrounding rock is squeezed—that is, non-squeezing deformation or
113 squeezing deformation. This study adopts the classification method of tunnel compression strength
114 commonly used in Hoek and Marinos (2000), Singh et al. (1992), and Aydan et al. (1993). The
115 deformation threshold for squeezing is $\varepsilon = 1\%$ (ε is the percentage strain), that is, when $\varepsilon > 1\%$,
116 the tunnel-surrounding rock will be squeezed. Among the 180 collected data samples, 112 were
117 non-squeezing samples and 68 were squeezing samples. In this paper, the code for the non-squeezing
118 condition is 0 and the code for the squeezing condition is 1.

119 **2.2 Data analysis**

120 To obtain the relationships between the parameters, a parameter interaction matrix was constructed, as
121 shown in Fig. 1(a). The graph on the diagonal in Fig. 1(a) shows the distribution of each individual
122 parameter (considering both squeezing and non-squeezing cases), while the graph not on the diagonal
123 shows their pairing relationship. Some outliers exist in Fig 1(a) that may lead to a lower classification
124 accuracy. Therefore, it is necessary to detect these outliers and perform denoising. Fig 1(b) shows the
125 correlation between the four parameters (*D*, *H*, *Q*, *K*) of the tunnel sample case after noise reduction.
126 The red lines in the non-diagonal graph below the diagonal are the nonlinear fitting lines for each
127 parameter pair.

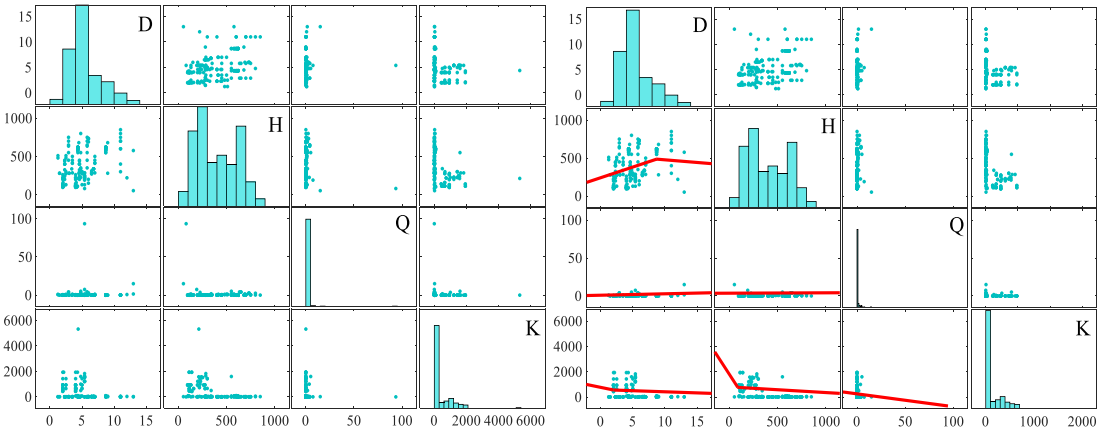

(a) Before denoising (b) After denoising

Fig. 1. Parameter interaction matrix

Fig. 2 shows the histogram, cumulative distribution and other statistical information (number of samples, maximum, minimum, average and standard deviation) of the four parameters (*D*, *H*, *Q*, *K*) used to predict tunnel squeezing. The database covers a wide range of the values of these four parameters; thus it has universality in principle. Based on the visualization principle of data association in Fig. 1, the No. 21 and No. 115 tunnel case samples (180 cases can be seen in the appendix) are eliminated, which is helpful for the later model analysis, and for establishing and improving the classification accuracy. Finally, 178 available samples are adopted.

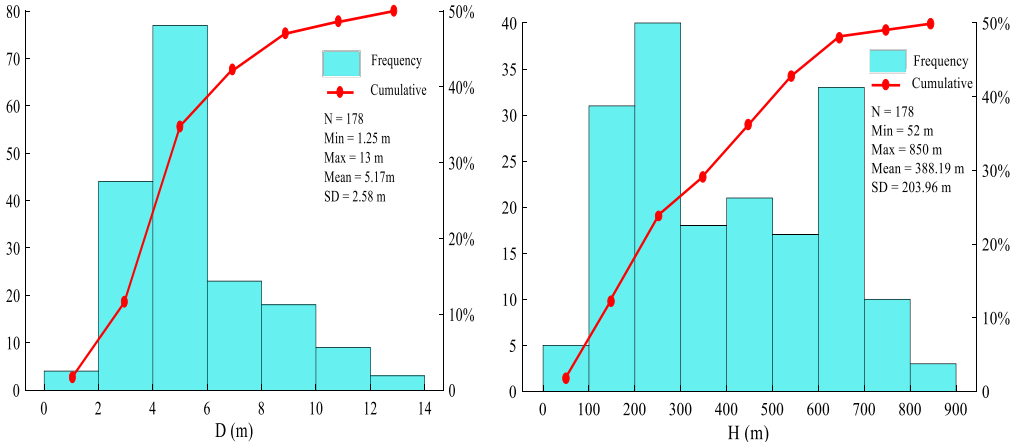

(a) *D* (b) *H*

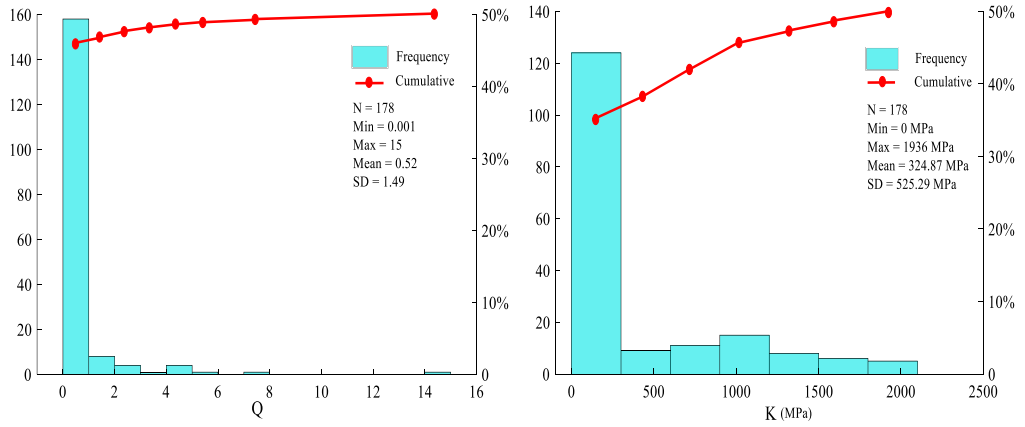

(c) Q (d) K

Fig. 2. The vertical and cumulative parameter distributions

3 Prediction model

3.1 SVM model

A support vector machine (SVM) is a machine learning algorithm in accordance to mathematical statistics theory. SVMs have been widely used in various industries because of their ability to solve problems such as high dimensionality and small sample sizes, nonlinearity and local minima (Dhakshina et al. 2020). In fact, the main feature of the support vector machine is that it uses a subset of the training set to represent a decision boundary, called a support vector, while the decision boundary is called the maximum edge hyperplane. The basic requirement of the SVM classifier is to find an optimal hyperplane to maximize the distance between the nearest point in space and itself, as shown in Fig. 3. The main idea of SVM can be divided into three problem categories: linearly separable, linearly inseparable and non-linearly separable.

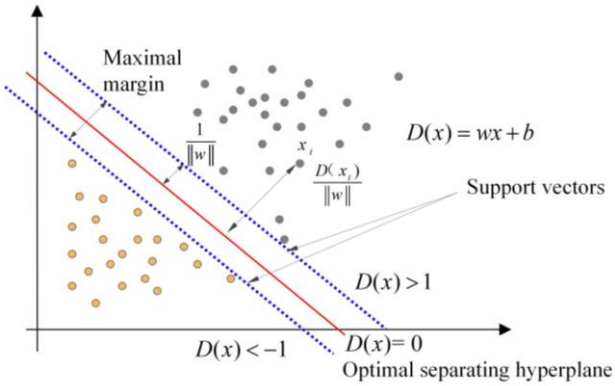

Fig. 3. Structure of a support vector machine

In this paper, predicting tunnel-surrounding rock squeezing is a nonlinear separable case that lies in the main purview of an SVM: that is, the samples cannot be classified by their linear relationship in a low dimensional space. By introducing a kernel function, a nonlinear transformation is presented to transform the input space correspond into a feature space where the hypersurface model in the input space corresponds to the hyperplane model in the feature space. In this way, the classification problem can be settled with a linear support vector machine applying to this high-dimensional feature space. Therefore, this paper mainly describes the nonlinear support vector machine.

Record *n* (here *n* = 178) known case observation samples as (u_1, v_1), (u_2, v_2), (u_n, v_n), where u_i is the characteristic parameter of the *i*-th tunnel case sample,, $u_i \in R^4$. A result of $v_i = -1$ indicates non-squeezing, while $v_i = 1$ indicates squeezing.

3.1.1 The sample is nonlinear and separable

First, we need to find an optimal hyperplane $w^T x + b = 0$, where w, $x \in R^4$, $b \in R^4$; w, b are undetermined and satisfy the following conditions (Chang and Lin, 2011):

$$\begin{cases} w^T u_i + b \geq 1, & v_i = 1 \\ w^T u_i + b \leq -1, & v_i = -1 \end{cases} . \quad (1)$$

Here, $v_i(wu_i - b) \geq 1$, where the sample that satisfies the equation $w^T u_i + b = \pm 1$ is called a support vector.

Then, to maximize the distance between the hyperplanes of the two types of data, we have (Chang and Lin, 2011):

$$\max \frac{2}{\|w\|} \Rightarrow \min \frac{1}{2}\|w\|^2 . \tag{2}$$

3.1.2 Establish the SVM model based on the RBF function

Step 1: define the generalized Lagrange function:

$$L(w,\alpha) = \frac{1}{2}\|w\|^2 + \sum_{i=1}^{n} \alpha_i \left[1 - v_i (w^T u_i + b)\right], \tag{3}$$

where $\alpha = (\alpha_1, \cdots, \alpha_n)^T$, $\alpha_i \geq 0$.

According to the Karush-Kuhn-Tucker complementary condition (Karush-Kuhn-Tucker, 2020), we can obtain partial derivatives of *w* and *b*:

$$\begin{cases} \dfrac{\partial L}{\partial w} = w - \sum_{i=1}^{n} \alpha_i v_i u_i = 0 \\ \dfrac{\partial L}{\partial b} = \sum_{i=1}^{n} \alpha_i v_i = 0 \end{cases}, \tag{4}$$

where $w = \sum_{i=1}^{n} \alpha_i v_i u_i$ and $\sum_{i=1}^{n} \alpha_i v_i = 0$ are acquired from the solution and are substituted into the original Lagrangian function to obtain the following functions:

$$L = \sum_{i=1}^{n} \alpha_i - \frac{1}{2} \sum_{i=1}^{n} \sum_{j=1}^{n} \alpha_i \alpha_j v_i v_j (u_i \cdot u_j), \tag{5}$$

where $(u_i \cdot u_j)$ is the linear form of the kernel function. By changing $(u_i \cdot u_j)$ into a general kernel function $K(x, y)$, we can obtain the general form of the model:

$$\max \sum_{i=1}^{n} \alpha_i - \frac{1}{2} \sum_{i=1}^{n} \sum_{j=1}^{n} \alpha_i \alpha_j v_i v_j K(u_i, u_j), \tag{6}$$

$$s.t. \begin{cases} \sum_{i=1}^{n} \alpha_i v_i = 0 \\ 0 \leq \alpha_i, i = 1, 2, \cdots, n \end{cases}. \tag{7}$$

Step 2: introduce the relaxation variable ξ, which allows a small number of samples to be incorrectly

divided. This method of processing is also called a soft interval. The parameter controlling the error level is c (Chang and Lin, 2011):

$$\min \frac{1}{2}\|w\|^2 + c\sum_{i=1}^{n}\xi_i , \tag{8}$$

$$s.t.\begin{cases} v_i(w^T u_i + b) \\ \xi_i \geq 0, i = 1,2,\cdots,n \end{cases} . \tag{9}$$

The classification function can be obtained by finding the optimal values for w^* and b^*:

$$f(x) = \mathrm{sgn}(w^{*T}x + b^*) . \tag{10}$$

3.1.3 Solution of SVM classification model

In this paper, 140 cases are taken as training samples, the optimization toolbox of MATLAB is used to solve steps 1 and 2 (described in Section 3.1.2), and the optimal solutions for w^* and b^* are obtained. The linear inseparable vector in the original sample space is transformed into a linearly separable vector in the high-dimensional feature space, and the optimal accuracy rate is obtained.

The remaining 38 cases are used as test samples $\tilde{u}_j,\ j = 1,2,\cdots,38$ for the classification function $f(x) = \mathrm{sgn}(w^{*T}x + b)$ in Eq. (10) and classified according to the following rules: $f(\tilde{u}_j) = -1$ indicates that the *j*-th sample point is a non-squeezing deformation; $f(\tilde{u}_j) = 1$ indicates that the *j*-th sample point is a squeezing deformation.

3.2 BP neural network model

Artificial neural networks (ANNs) constitute a new, interdisciplinary, and widely used field. They are based on a simplified simulation of the human brain's neural system, which is composed of a large number of adaptive processing units that are densely connected to each other. This approach can also be considered a processing system for large-scale information. The BP neural network is a multilayer feedforward neural network trained by an error back-propagation algorithm, making it a mainstream

type of neural network. The main characteristic of the error back-propagation algorithm is that the sample is input in the forward direction, while errors are back-propagated to update the network (Zhou, 2016). The error back-propagation is mainly based on the strategy of gradient descent to improve the model weights and thresholds causing the output of the model to be successively closer to the expected output. The steps of the BP neural network algorithm are as follows:

Step 1: Construct the neural network and initialize it

Based on the characteristic parameters and output categories of each group of data, a three-layer BP neural network is set up that contains a d input node and a q output node. According to the Kolmogorov theorem, the number of hidden layer nodes is represented by v, and $v = 2d + 1$. The smaller random number is selected as the connection weight w_{im} between the input layer and the hidden layer and the initial value of the connection weight w_{mj} between the hidden layer and the output layer. The selection rules for the initial values of the thresholds ϕ_m and θ_j of the neurons in the hidden layer and the output layer are the same. w_{im} is the connection weight between the *i*-th neuron in the input layer and the *m*-th neuron in the hidden layer, and w_{mj} is the connection weight between the *m*-th element in the hidden layer and the *j*-th neuron in the output layer. ϕ_m is the threshold of the *m*-th neuron in the hidden layer, and θ_j is the threshold of the *j*-th neuron in the output layer. Finally, the activation functions f and f' are set for the hidden layer and output layer, respectively, and the learning rate η is set.

Step 2: Calculate the output value and the error value of the output layer.

$$P_m = f\left(\sum_{i=1}^{d} w_{im} x_i - \phi_m\right), \tag{11}$$

where $P_m (m = 1, 2, \cdots, v)$ is the output value of the *m*-th neuron in the hidden layer and x_i is the *i*-th characteristic parameter of each group of data:

$$y_j = f^{'}(\sum_{m=1}^{v} w_{mj} P_m - \theta_j), \tag{12}$$

where $y_j (j = 1, 2, \cdots, q)$ is the predicted output value of the *j*-th neuron in the output layer:

$$e_j = Y_j - y_j, \tag{13}$$

and $Y_j (j = 1, 2, \cdots, q)$ is the ideal output value of the *j*-th neuron in the output layer, and $e_j (j = 1, 2, \cdots, q)$ is the prediction error value of the *j*-th neuron in the output layer.

Step 3: Adjust the connection weight and threshold.

Based on the principle of gradient descent, the relevant parameters are adjusted in the backward direction. The adjustment formula for any related parameter λ is (Zhou, 2016):

$$\lambda \leftarrow \lambda + \Delta\lambda. \tag{14}$$

The weights and thresholds are adjusted as follows (Wang and Shi, 2013) [28]:

$$w^{'}_{im} = w_{im} + \eta P_m (1 - P_m) x_i \sum_{j=1}^{q} w_{mj} e_j, \tag{15}$$

$$w^{'}_{mj} = w_{mj} + \eta P_m e_j, \tag{16}$$

$$\phi^{'}_{m} = \phi_m + \eta P_m (1 - P_m) \sum_{j=1}^{q} w_{mj} e_j, \tag{17}$$

$$\theta^{'}_{j} = \theta_j + e_j. \tag{18}$$

Step 4: Repeat the above steps during the training process of the neural network, which can be considered as a process searching for the optimal parameter solutions—that is, minimize *e* by finding a set of optimal parameters in the parameter space. This process can be expressed as follows: when an $e(\omega_{im}, \omega_{mj}, \phi_m, \theta_j) \geq e(\omega^*_{im}, \omega^*_{mj}, \phi^*_m, \theta^*_j)$ exists for any $(\omega_{im}, \omega_{mj}, \phi_m, \theta_j)$ in the parameter space; then, $(\omega^*_{im}, \omega^*_{mj}, \phi^*_m, \theta^*_j)$ is the global minimum solution. Fig. 4 shows the basic steps involved in training the BP neural network.

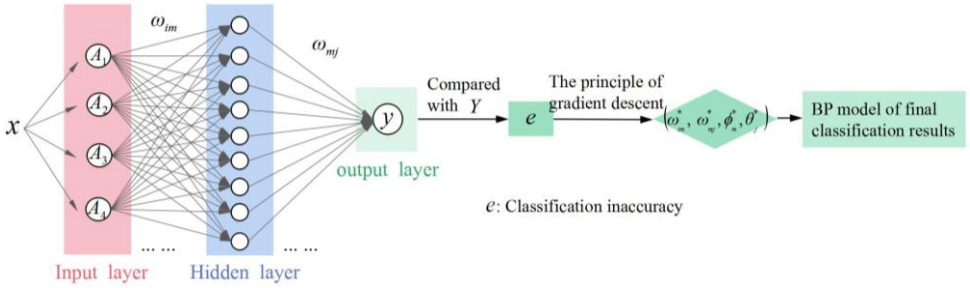

Fig. 4. Basic structure and step diagram of the BP neural network

3.3 SVM-BP combination model

Many scholars use single classification methods (such as a clustering analysis of Euclidean distance, logistic regression analysis, support vector machine, naive Bayes or other classification method) to evaluate and predict the squeezing of surrounding rock. Due to the different emphases of different classifiers, each individual classification method has certain limitations. In addition, the performance of a single classifier trained by a standard learning algorithm differs on different data sets; the same classifier can also show different performances on different test sets (Samadzadegan, et al. 2010). For example, (Jimenez and Recio, 2011) reported that the log$Q$ vs log$H$ linear classifier model reduces the number of classification errors; (Feng and Jimenez, 2015) showed that it is more advantageous to use the BN model to determine the weights of various indicators when the input data are incomplete.

However, some studies show that the performance of multi-classifier fusion methods is better than that of single classifiers. For example, (Zhao and Liu, 2020) reported that the advantage of using a combination method involving multiple classifiers is that it results in a more stable performance on different data sets. This advantage is also significant for improving the overall system performance. The research of Sun et al. (2018) showed that the performance of the DAG-SVM multi-classifier fusion is better than that of a classical binary SVM classifier for non-squeezing classification. Chen et al. (2020) considered that a combined classifier consisting of the Bayesian algorithm and a Markov geological model after training a decision tree achieves higher prediction accuracy than does a single

classifier. However, in the field of surrounding rock squeezing classification, research using multi-classification fusion approaches is still limited; consequently, this line of research needs to be further expanded.

Therefore, this paper proposes an SVM-BP combination model by fusing the complementary advantages of an SVM and a BP neural network. Using an application involving the classification of surrounding rock squeezing, the classification performance differences between the SVM and BP model and the advantages and disadvantages of the combined SVM-BP model are explored. The SVM-BP combination model is constructed as follows:

First, in this study, based on 178 sets of original characteristic parameter sets of tunnel and surrounding rock where each group has four characteristic parameters $A_i(i=1,2,\cdots,4)$, a three-layer BP neural network is set up containing four nodes in the input layer and four nodes in the hidden layer. The input value and the output target value are four original feature parameters $p_{ji}\left(j=1,2,\cdots,4,i=1,2,\cdots,178\right)$, and the number of hidden layer nodes corresponds to the number of new feature parameters. The nonlinear mapping ability of the BP neural network is used to transform the features in the sample data, the characteristic parameters are mapped to the new feature parameter space, and the linearly separable feature parameters are obtained.

Then, when the learning error e satisfies condition $e=\sum_{i=1}^{178}\sum_{j=1}^{4}\left(p_{ji}^{'}-p_{ji}\right)\le r$, the weights and thresholds of the modified BP neural network are the best mapping relations for feature extraction, and the output value of the hidden layer is the new feature parameter $p_{ji}^{'}$.

Finally, after the feature extraction of the tunnel-surrounding rock squeezing is completed, the classification and recognition of tunnel-surrounding rock squeezing is carried out. Because of the strong generalizability of the SVM, the transformed features are input into the SVM classifier for

reinforcement learning, which overcomes the poor generalization ability of the BP neural network. By using the RBF kernel function, the data processed by the BP neural network are mapped from the input space to the high-dimensional feature space, and a linear separable vector is obtained. The feature parameters fully reflect the classification hyperplane effect of the SVM classifier and obtain the best classification accuracy. The working principle of the SVM-BP model is shown in Fig. 5.

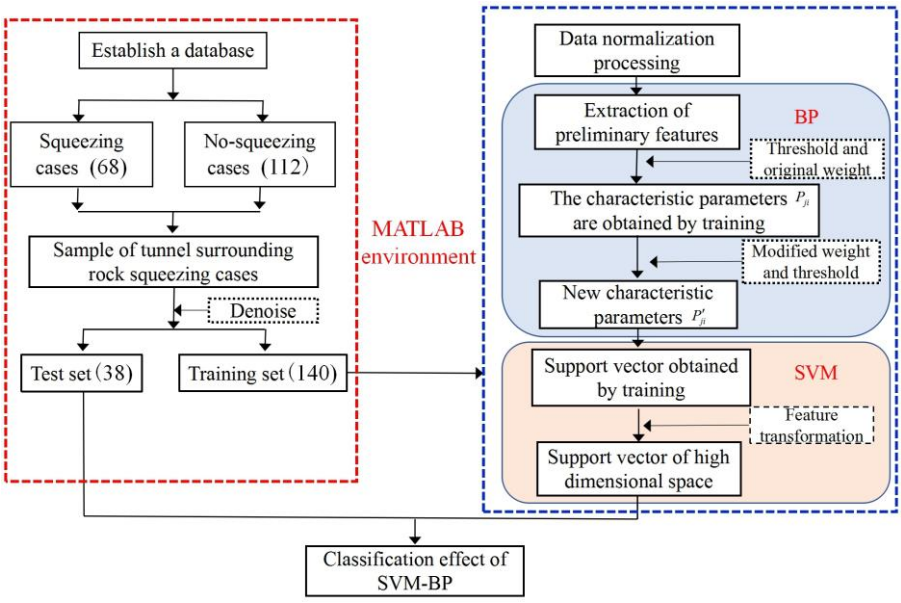

Fig. 5. Process of large scale prediction based on the SVM-BP classifier model

4 Results and analysis

The innovation of this study is to present a combined model based on both an SVM and a BP model and applied to classify tunnel-surrounding rock squeezing. In particular, this study was designed to further analyse the accuracy of the model prediction results and the influence of feature parameters on the prediction results by combining different feature parameters and using three classifiers (SVM, BP, and the SVM-BP combination model). In addition, we compared our combined model with other previously reported prediction methods to verify its reliability.

4.1 Prediction accuracy analysis

Fig. 6 shows the prediction accuracy of the SVM, BP and the SVM-BP combination model when the

characteristic input parameters are D, H, Q and K. As Fig. 6 shows, all three models have good prediction accuracy. However, the maximum accuracy rate of the SVM-BP combination model is 92.11%, which is better than that of the SVM model (89.47%) and the BP model (89.47%). The results show that the combination SVM-BP classifier achieves better performances than do the single SVM or BP neural network classifiers when classifying tunnel-surrounding rock squeezing; on average, the SVM-BP classifier improves the accuracy rate by 2.64%. The fusion of multiple classifiers can compensate for the shortcomings of a single classifier to a certain extent, helping to achieve higher classification accuracy. Fig. 7 presents confusion matrices for the BP and SVM-BP model, showing that the accuracy rate of the SVM-BP model for predicting surrounding rock squeezing is slightly higher than that of the non-squeezing case. The accuracy rate of the BP model in predicting the surrounding rock squeezing is consistent with that of the non-squeezing case. However, its error rate for predicting a non-squeezing case as a squeezing case is higher. Generally, the accuracy of the SVM-BP model to predict the surrounding rock squeezing is higher than that of the BP model. For surrounding rock non-squeezing, the BP model is slightly superior to the SVM-BP model; however, it should be noted that the prediction results are affected by the quantity of test set samples, and the greater the number of test set samples, the more obvious the differences in model performance may be.

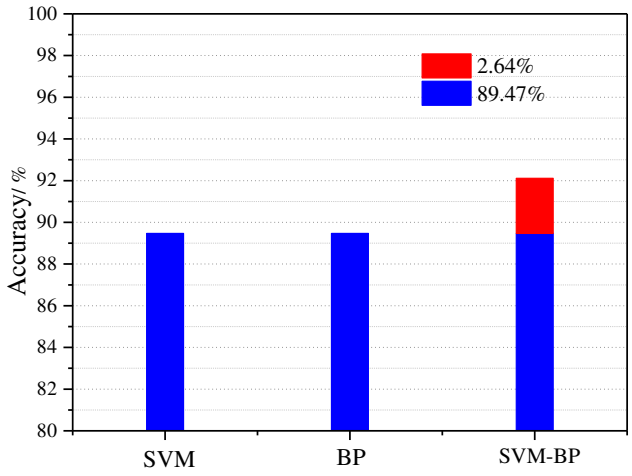

Fig. 6. Comparison of the classification results of three classifiers

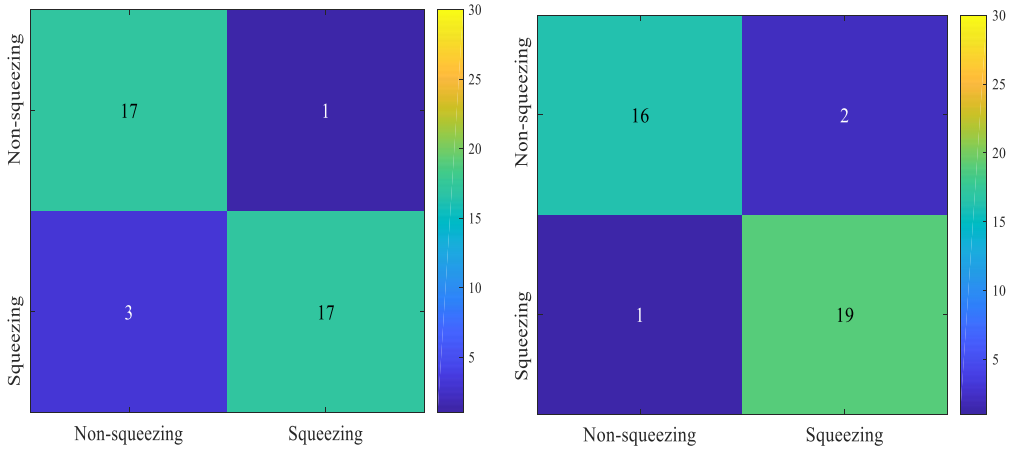

(a) BP (b) SVM-BP

Fig. 7. Confusion matrices for the BP and SVM-BP models

Fig. 8 shows the prediction performances of the three models on the test set. The SVM-BP model reaches the highest accuracy index value of 0.92, which is 0.26 higher than that of the SVM model and BP model. The Kappa index value of the SVM-BP model is also the highest (0.89), followed by the BP model (0.80), while that of the SVM is the worst (0.78). According to the results of the test set, based on the four indicators *H*, *D*, *Q*, and *K*, the SVM-BP model also achieves the best prediction performance, recall rate = 0.95 and F1 = 0.92. F1-value was presented to show the advantages and disadvantages of various algorithms, which was based on both precision and recall and could evaluate precision and recall as a whole. The F1 value = precision × recall × 2/(precision + recall).

Fig. 9 shows a comparison of the AUC values of the three models after 10 iterations on the test set. The area under the curve (AUC) is the area under the receiver operating characteristic (ROC) curve. The reason why the AUC value is usually used as a model evaluation standard is that the ROC curve does not clearly show which classifier is better. In contrast, as a numerical value, a higher AUC value indicates a better classifier. Fig. 9 shows that the AUC value of SVM-BP is the highest (0.92), and that the AUC values of SVM and BP are 0.89. Therefore, the classification effect of the SVM-BP model is

346 better.

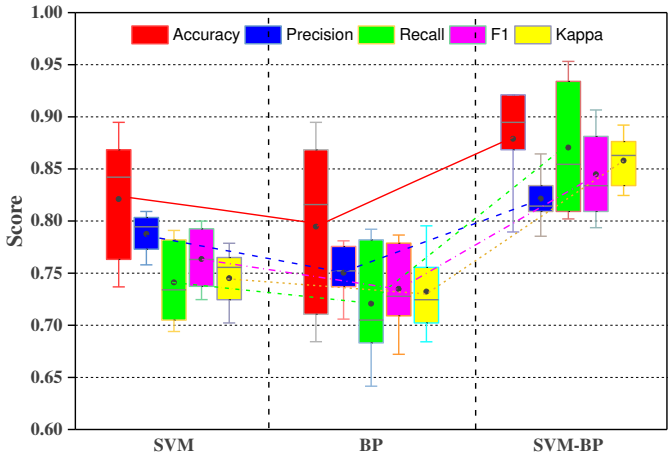

347

348 Fig. 8. Comparison of the prediction performance indexes of three classifiers

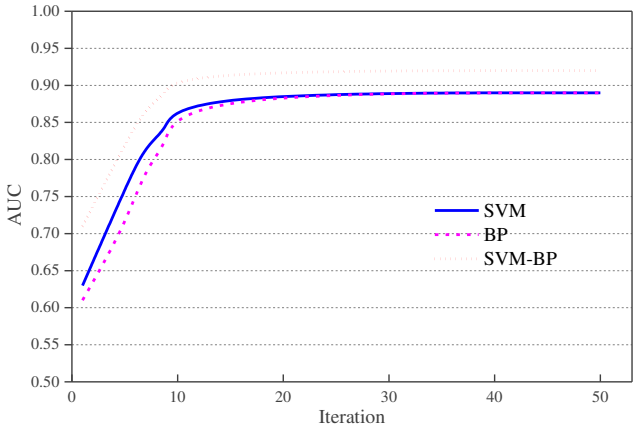

349

350 Fig. 9. Comparison of the AUC values of three classifiers

351 **4.2 Prediction method analysis**

352 To compare and analyse the performance of the SVM-BP combination model and other classification

353 methods reported in the literature, the performance of the SVM-BP combination model in surrounding

354 rock deformation classification is analysed. Table 2 shows a summary of the other existing methods

355 and the combined method proposed in this paper, while Fig. 10 shows the accuracy comparison results

356 of the various existing methods and the combined method proposed in this paper.

357 Table 2. Classification comparison between the methods in this paper and other models in the literature

Indicators of	Shafiei, et	Feng, et al	Sun, et al	Chen, et al	Zhang, et al	The method

comparison	al (2012)	(2015)	(2018)	(2020)	(2020)	of this paper
Number of case samples	198	166	117	154	166	178
Prediction parameters	*H, Q*	*H, D, Q, K, SSR*	*H, D, Q, K*	*H, K, SSR, GC, D*	*H, D, Q, K, SSR*	*H, D, Q, K*
Prediction method	SVM	BN	M-SVM	DT	SVM, ANN, KNN, DT, LR, MLR, NB	SVM-BP
Accuracy/%	84.10	86.65	84.10	93.50	96.00	92.11
Number of classifiers	1	1	1	3	7	2
Advantages	A certain accuracy can be achieved based on fewer indicators	It can predict the large scale probability	The degree and probability of surrounding rock extrusion deformation can be calculated	It can dynamically predict the squeezing probability of rock	High accuracy	The model is simple and universal

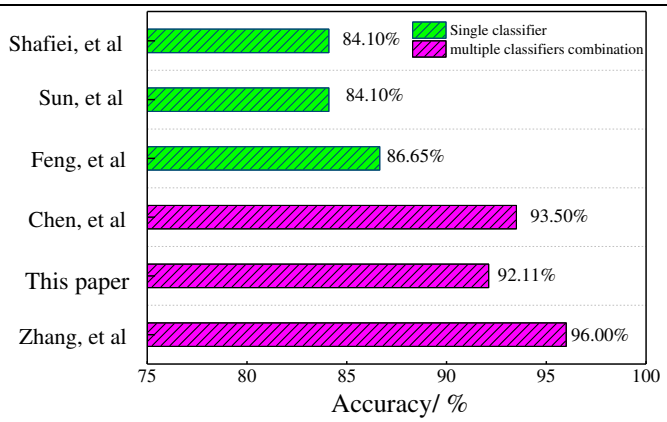

Fig. 10. Comparison of classification accuracy between the proposed method and methods proposed in previous studies

Table 2 and Fig. 10 show that in terms of the performance of a single classifier, Shafiei et al. (2012) constructed an SVM model based on two indexes (*H* and *Q*) to classify the surrounding rock squeezing that reached an overall accuracy rate of 84.1%; Sun et al. (2018) constructed an M-SVM (multi class

364 support vector machine) model based on the four indicators (*D*, *H*, *Q*, and *K*) to classify the
365 surrounding rock squeezing that achieved an overall accuracy of 84.1%. The accuracy of the model
366 proposed in this paper is slightly higher than that of Shafiei et al. (2012) when the same SVM model is
367 used and the number of case samples is similar; this result may be related to the number of indicators.
368 The coupling effect of the four indicators is clear.
369 In terms of the performance of multiple classifier combinations, the SVM-BP model proposed in this
370 paper is compared with Chen et al. (2020) which uses a decision tree combined with Bayesian updating,
371 the Markov chain model, and with Zhang et al. (2020) model, which uses a weighted combination of
372 seven classifier models. The common point among all these models is that the performances of the
373 three multi-classifier combination models are considerably higher than those of any single classifier.
374 Chen et al. (2020) achieves an accuracy rate of 93.5%, Zhang et al. (2020) achieved an accuracy rate of
375 96%, and the accuracy of the model proposed in this paper is 92.11%. The emphases of these
376 combination models are different. The method in this paper focuses on the classification of statistical
377 case data. The disadvantage of the proposed SVM-BP model is that it cannot dynamically predict the
378 surrounding rock squeezing; however, the model is relatively simple and achieves high accuracy. Chen
379 et al. (2020) focused predicting surrounding rock squeezing probability based on time series and
380 established a model that integrated a decision tree with Bayesian updating and Markov geology to
381 predict the probability of surrounding rock squeezing; however, that model is relatively difficult to
382 control. Zhang et al. (2020) focused on determining the weights of seven classifiers predicting the
383 deformation of surrounding rock and established seven weighted combination models of classifiers,
384 including SVM, ANN, KNN, DT, LR, MLR and NB, to classify the surrounding rock squeezing. The
385 classification accuracy rate of this combined model reaches as high as 96%, and it greatly improves the

386 classification accuracy. However, when the number of classifiers is too large, the focus of classification
387 is not obvious; thus, this method is too complex, theoretical and not universal.

388 **4.3 Parameter impact analysis**

389 This section mainly discusses the reliability and applicability of the SVM, BP and SVM-BP models in
390 predicting tunnel squeezing with fewer prediction parameters. We combined the four parameters (*D*, *H*,
391 *Q*, and *K*). The prediction accuracies of the different models are shown in Table 3. Table 3 shows that
392 the accuracy with the four combined parameters (*D*, *H*, *Q*, and *K*) is the highest: 89.47% (SVM),
393 89.47% (BP) and 92.11% (SVM-BP), respectively. Therefore, the above four parameters can be used
394 to predict tunnel-surrounding rock squeezing. The results show that the accuracy of the SVM-BP
395 combination model is 89.47% while the prediction accuracy of the BP neural network is 86.84% when
396 *D*, *H*, and *Q* are used to classify the surrounding rock squeezing. However, as a single classifier, the
397 SVM achieves a higher prediction accuracy (86.84%) when using the *D*, *H*, and *K* parameters. In
398 contrast, the prediction accuracy of the SVM-BP combination model based on the *D*, *Q*, and *K*
399 parameters is only 86.84%, which is better than that of the single classifier. Based on only the
400 parameters *H*, *Q* and *K*, the prediction results of the three models are not ideal, but again, the prediction
401 accuracy of the SVM model is the highest, at 76.32%. Therefore, different parameters are most suitable
402 for different classifiers.

403 In addition, the comparison of the prediction results when using the *D*, *H*, *Q*, *K* and the *H*, *Q*, *K*
404 parameters shows that the prediction accuracy of the three models is greatly reduced; in fact, the
405 prediction accuracy of the SVM-BP model decreases from 92.11% to 60.53%, the most significant
406 decrease. This shows that the tunnel diameter *D* is the most important parameter in predicting the
407 surrounding rock squeezing, which is consistent with the conclusion reached by Chen et al. (2020).

Among the four characteristic parameters, *H* has the least influence on tunnel-surrounding rock squeezing prediction. However, the results of this model do not reflect the influence of *Q* and *K* parameters on the overall accuracy. Therefore, we use variance analysis to verify the significance of *D*, *Q* and *K* parameters. The significance values of *D*, *K* and *Q* parameters are 0.000, 0.001 and 0.104, respectively, indicating that *K* and *D* have a significant influence on the surrounding rock squeezing. This conclusion is consistent with the results of Feng et al. (2015), Sun et al. (2018), Chen et al. (2020), Zhang et al. (2020), and further verifies the feasibility of the SVM-BP model in this paper.

Table 3. Comparison of accuracy results of three classifiers

Prediction parameters	Accuracy/%		
	SVM	BP	SVM-BP
D, H, Q, K	89.47	89.47	92.11
D, H, Q	71.05	86.84	89.47
D, H, K	86.84	84.21	86.84
D, Q, K	78.95	76.32	86.84
H, Q, K	76.32	65.79	60.53

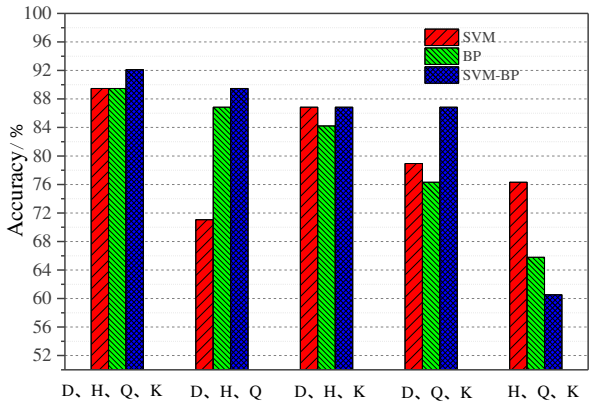

Fig. 11. Comparison of the classification accuracy of the three classifiers

5 Conclusion and discussion

(1) This study constructed an SVM-BP combination model to classify tunnel-surrounding rock squeezing by using four characteristics: *D*, *H*, *Q*, and *K*. The proposed model achieves a classification accuracy as high as 92.11%. The SVM-BP combination model is both simple and reliable.

(2) In classifying surrounding rock squeezing, through a comparison of three classifiers, this study

concludes that the SVM-BP model combines the advantages of an SVM and a BP neural network; and that the combined model has flexible nonlinear modelling and parallel processing capabilities for large-scale data. Thus, the SVM-BP model achieves better classification performances than do the SVM and BP models. Simultaneously, however, the combined model may also reflect the shortcomings of both because its effect is not good on some classification problems. This aspect of the results is worth further study and mining.

(3) In this study, three classifiers (SVM, BP, SVM-BP) were used to classify tunnel-surrounding rock squeezing. Because this is a two classification problem, the accuracy of all three tested classifiers is high. At present, most of the methods classify their results into two categories; however, in the future, predicting the probability of tunnel-surrounding rock squeezing has more practical significance.

(4) By combining different characteristic parameters and using different models to classify the surrounding rock squeezing, it can be concluded that the coupling of D, H and K has a large influence on the prediction of surrounding rock squeezing under different models.

(5) In future work, we plan to further study how to select the optimal feature subset by using optimization techniques to improve the performance of multi-classifier combinations.

Conflicts of Interest

The authors declare that there are no conflict of interest.

Acknowledgements

This work was supported by the National Science Foundation of China (Grant Nos. 51978668, 51968005), and the Guangxi University Young and Middle-Aged Teachers' Basic Scientific Research Ability Improvement Project (2020ky01011).

References

445 Aydan, Ö., Akagi, T., Kawamoto, T., 1996. The squeezing potential of rock around tunnels: theory and
446 prediction with examples taken from japan. Rock Mechanics & Rock Engineering. 26, 137–163.
447 https://doi.org/10.1007/BF01032650.
448 Chang, C. C., Lin, C. J., 2011. Libsvm: a library for support vector machines. ACM Transactions on
449 Intelligent Systems and Technology. 2(3), 1–27. https://10.1145/1961189.1961199.
450 Chen, Y., Li, T. B., Zeng, P., Ma, J. J., Patelli, E., Edwards, B., 2020. Dynamic and probabilistic
451 multi-class prediction of tunnel squeezing intensity. Rock Mechanics and Rock Engineering. 53,
452 3521-3542. https://10.1007/s00603-020-02138-8.
453 Debernardi, D., Barla, G., 2009. New viscoplastic model for design analysis of tunnels in squeezing
454 conditions. Rock Mechanics and Rock Engineering. 42(2), 259.
455 https://doi.org/10.1007/s00603-009-0174-6.
456 Dhakshina K., Esakkirajan, S., Bama, S., Keerthiveena, B., 2020. A microcontroller based machine
457 vision approach for tomato grading and sorting using SVM classifier. Microprocessors and
458 Microsystems. 76, 103090. https://doi.org/10.1016/j.micpro.2020.103090.
459 Ding, S., Su, C., Yu, J., 2011. An optimizing BP neural network algorithm based on genetic algorithm.
460 Artificial Intelligence Review. 36(2), 153-162. https://doi.org/10.1007/s10462-011-9208-z.
461 Dwivedi, R. D., Singh, M., Viladkar, M. N., Goel, R. K., 2013. Prediction of tunnel deformation in
462 squeezing grounds. Engineering Geology. 161, 55-64.
463 https://doi.org/10.1016/j.enggeo.2013.04.005.
464 Feng, X. D., Jimenez, R., 2015. Predicting tunnel squeezing with incomplete data using bayesian
465 networks. Engineering Geology. 195, 214-224. https://doi.org/10.1016/j.enggeo.2015.06.017.
466 Fritz, P. , 2010. An analytical solution for axisymmetric tunnel problems in elasto-viscoplastic media.
467 International Journal for Numerical & Analytical Methods in Geomechanics. 8(4), 325-342.
468 https://doi.org/10.1002/nag.1610080403.
469 Gao, F., Stead, D., Kang, H., 2015. Numerical simulation of squeezing failure in a coal mine roadway
470 due to mining-induced stresses. Rock Mechanics and Rock Engineering. 48(4), 1635-1645.
471 https://doi.org/10.1007/s00603-014-0653-2.
472 Ghasemi, E., Gholizadeh, H., 2018. Development of two empirical correlations for tunnel squeezing
473 prediction using binary logistic regression and linear discriminant analysis. Geotechnical and
474 Geological Engineering. 37(4), 3435-3446. https://doi.org/10.1007/s10706-018-00758-0.

Goel, R. K., Jethwa, J. L., Paithankar, A. G.,1995. Tunnelling through the young himalayas — a case history of the maneri-uttarkashi power tunnel. Engineering Geology. 39(1-2), 31-44. https://doi.org/10.1016/0013-7952(94)00002-J.

Hoek, E., Marinos, P., 2000. Predicting tunnel squeezing problems in weak heterogeneous rock masses. Tunnels and Tunnelling International. 32(11)，45-51+33-36.

Hoek, E., 2001. Big tunnels in bad rock. Journal of Geotechnical and Geoenvironmental Engineering. 127(9), 726-740. https://doi.org/10.1061/(ASCE)1090-0241(2001)127:9(726).

Jethwa, J. L., Singh, B., Singh, B., 1984. Estimation of ultimate rock pressure for tunnel linings under squeezing rock conditions — a new approach. Proccedings of ISRM Symposium on Design and Performance of Underground Excavations. 22(1), 231–238. https://doi.org/10.1016/0148-9062(85)92771-8.

Jimenez, R., Recio. D., 2011. A linear classifier for probabilistic prediction of squeezing conditions in Himalayan tunnels. Engineering Geology. 121, 101–109. https://doi.org/10.1016/j.enggeo.2011.05.006.

Karush-Kuhn-Tucker, 2020, (Access online: http://apmonitor.com/me575/index.php/Main/KuhnTucker)

Mahdevari, S., Haghighat, H. S., Torabi, S. R., 2013. A dynamically approach based on svm algorithm for prediction of tunnel convergence during excavation. Tunnelling and Underground Space Technology. 38(9), 59-68. https://doi.org/10.1016/j.tust.2013.05.002.

Samadzadegan, F., Bigdeli, B., Ramzi, P., 2010. A multiple classifier system for classification of LIDAR remote sensing data using multi-class SVM. 9th International Workshop on Multiple Classifier Systems, Cairo, EGYPT , 5997, 254-263.

Shafiei, A., Parsaei, H., Dusseault, M. B., 2012. Rock squeezing prediction by a support vector machine classifier. 46th US Rock Mechanics / Geomechanics Symposium 2012. Chicago. USA.

Singh, B., Jethwa, J. L., Dube, A. K., Singh, B., 1992. Correlation between observed support pressure and rock mass quality. Tunnelling and Underground Space Technology. 7(1), 59–74. https://doi.org/10.1016/0886-7798(92)90114-W.

Singh, B., Goel, R., K., Jethwa, J. L., 1997. Support pressure assessment in arched underground openings through poor rock masses. Engineering Geology. 48(1-2), 59–81. https://doi.org/10.1016/S0013-7952(97)81914-X.

505 Sun, Y., Feng, X., Yang, L., 2018. Predicting tunnel squeezing using multiclass support vector
506 machines. Advances in Civil Engineering. 2018, 4543984. https://doi.org/10.1155/2018/4543984.
507 Wang, J., 2020. The Key Way is to Release the Genuine Rock Pressure—Discussion on problems of
508 tunnelling in squeezing ground. Modern Tunnelling Technology. 57(4), 1-11.
509 Wen, J., Li, Z. J., Wei, L. S., Zhen, H., 2002. The improvements of BP neural network learning
510 algorithm. IEEE: 16th World Computer Congress 2000. Beijing. China, 1647-1649.
511 https://doi.org/10.1109/ICOSP.2000.893417.
512 Yassaghi, A., Salari-Rad, H., 2005. Squeezing rock conditions at an igneous contact zone in the Taloun
513 tunnels, Tehran-Shomal freeway, Iran: a case study. International Journal of Rock Mechanics and
514 Mining Sicences. 42(1), 95-108. https://doi.org/10.1016/j.ijrmms.2004.07.002.
515 Zhang, J., Li, D., Wang, Y., 2020. Predicting tunnel squeezing using a hybrid classifier ensemble with
516 incomplete data. Bulletin of Engineering Geology and the Environment. 79(6), 3245-3256.
517 https://doi.org/10.1007/s10064-020-01747-5.
518 Zhao, H. H., Liu, H., 2020. Multiple classifiers fusion and CNN feature extraction for handwritten
519 digits recognition. Granular Computing. 5(3), 411-418.
520 https://doi.org/10.1007/s41066-019-00158-6.
521 Zhou, G., Sun, Y., Peng, J., 2018. Application of genetic algorithm based BP neural network to
522 parameter inversion of surrounding rock and deformation prediction. Modern Tunnelling
523 Technology. 55(01), 107-113. https://doi.org/10.13807/j.cnki.mtt.2018.01.015.
524 Zhou, Z.H., 2016. Machine Learning. Tsinghua University Press, Beijing, China.

Figures

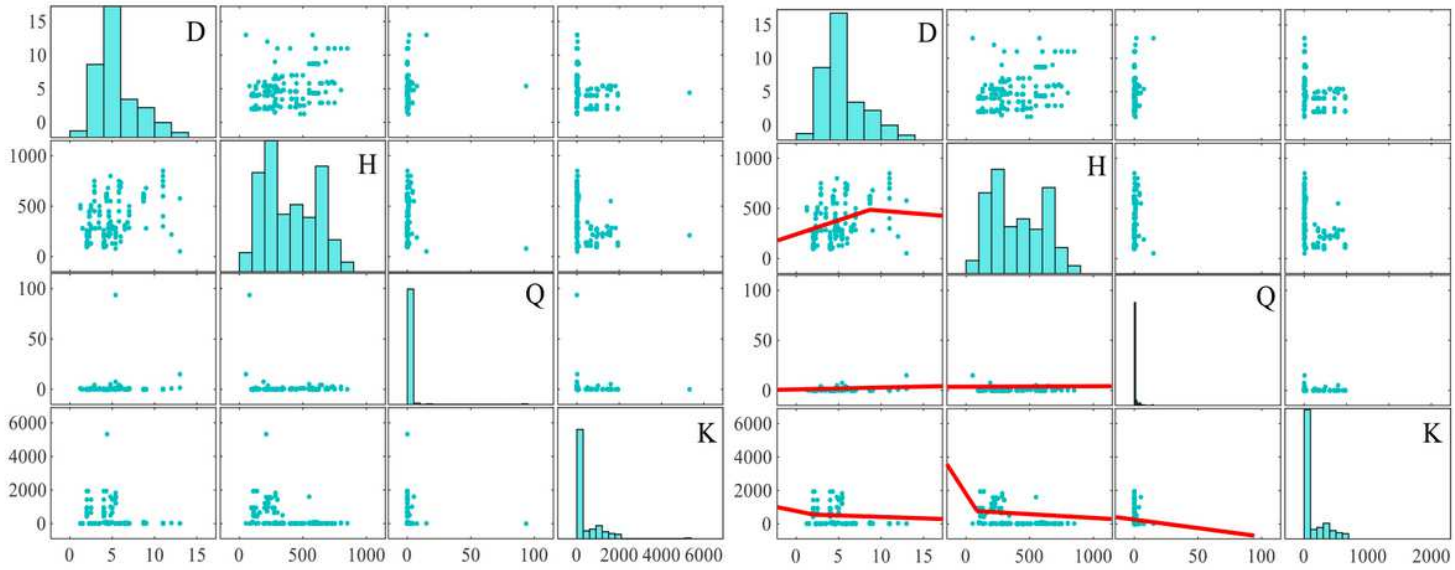

Figure 1

Parameter interaction matrix

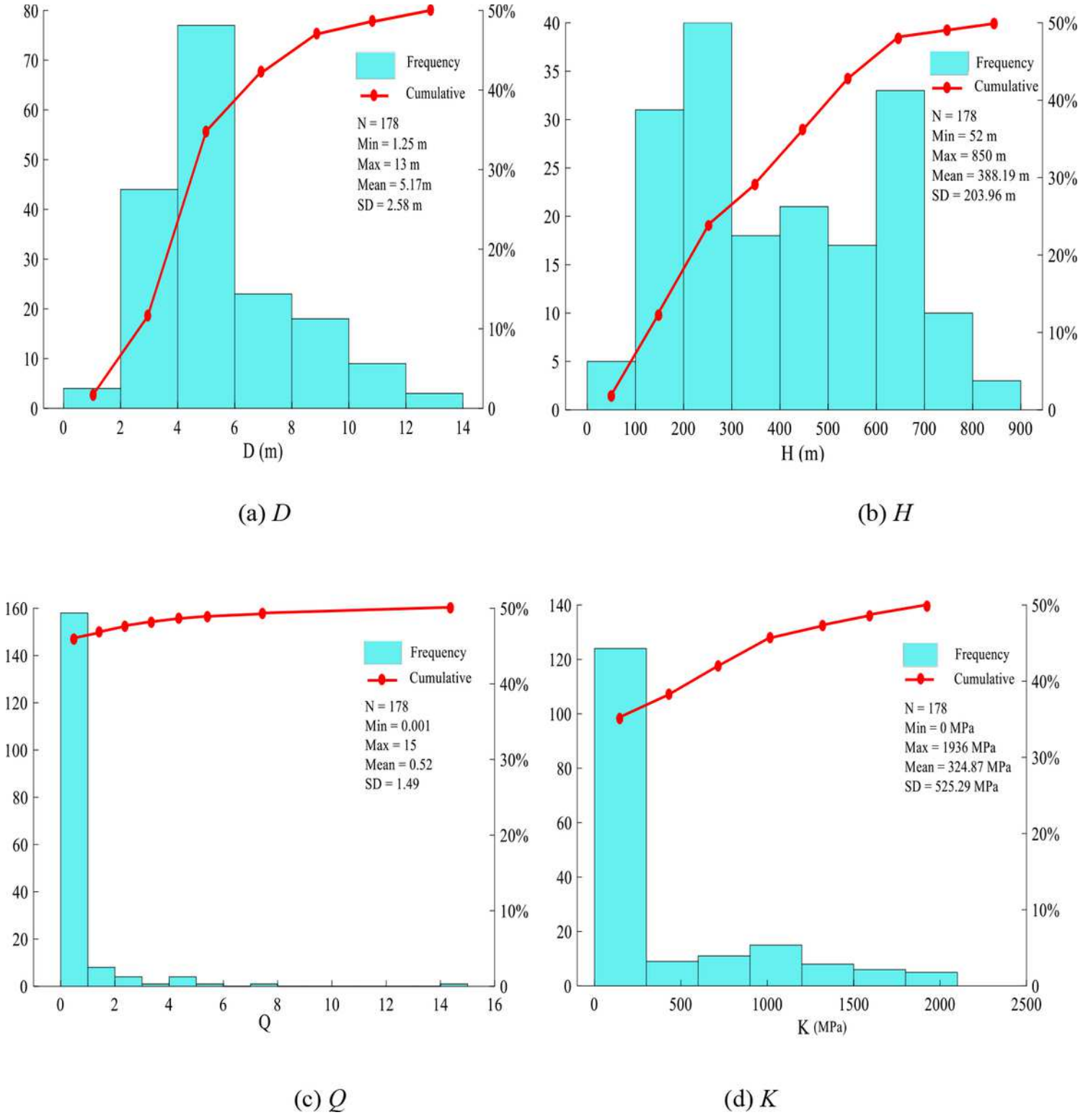

Figure 2

The vertical and cumulative parameter distributions

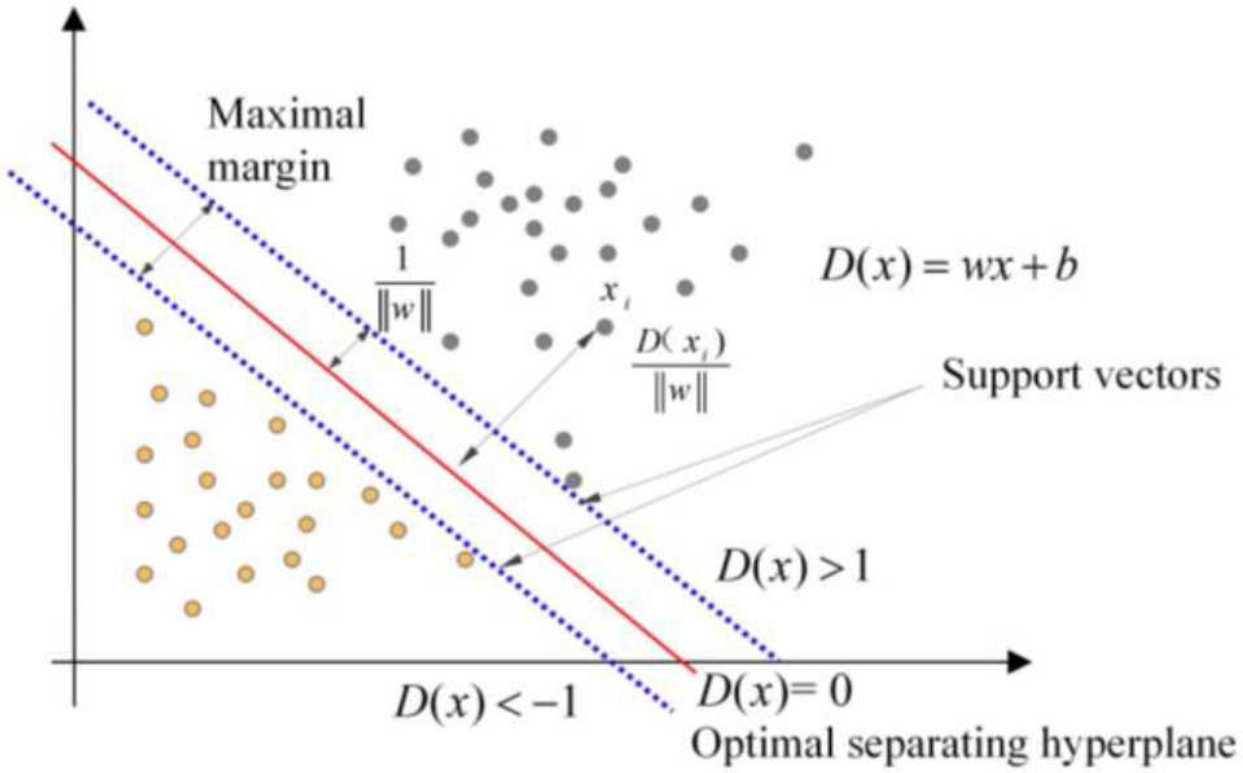

Figure 3

Structure of a support vector machine

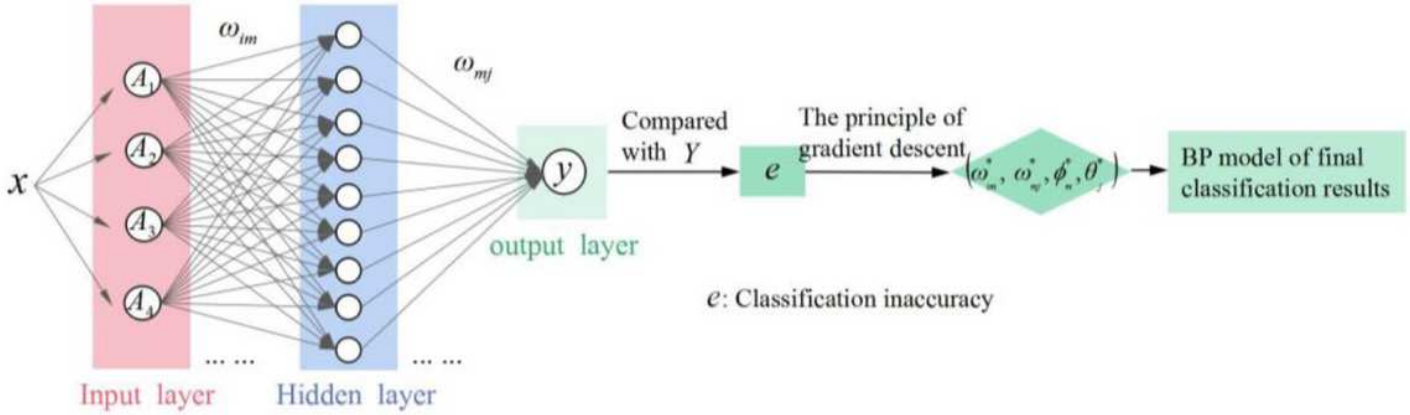

Figure 4

Basic structure and step diagram of the BP neural network

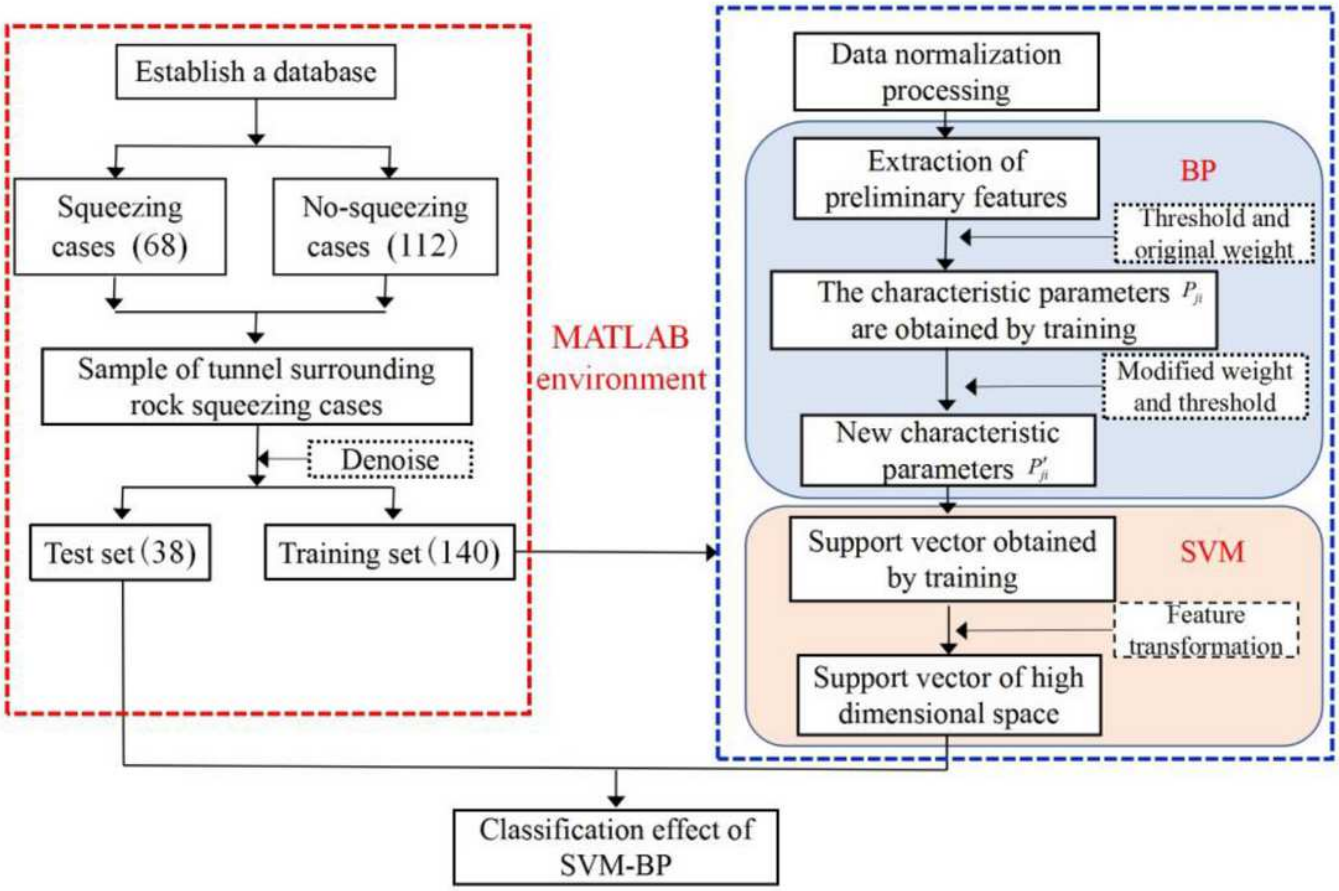

Figure 5

Process of large scale prediction based on the SVM-BP classifier model

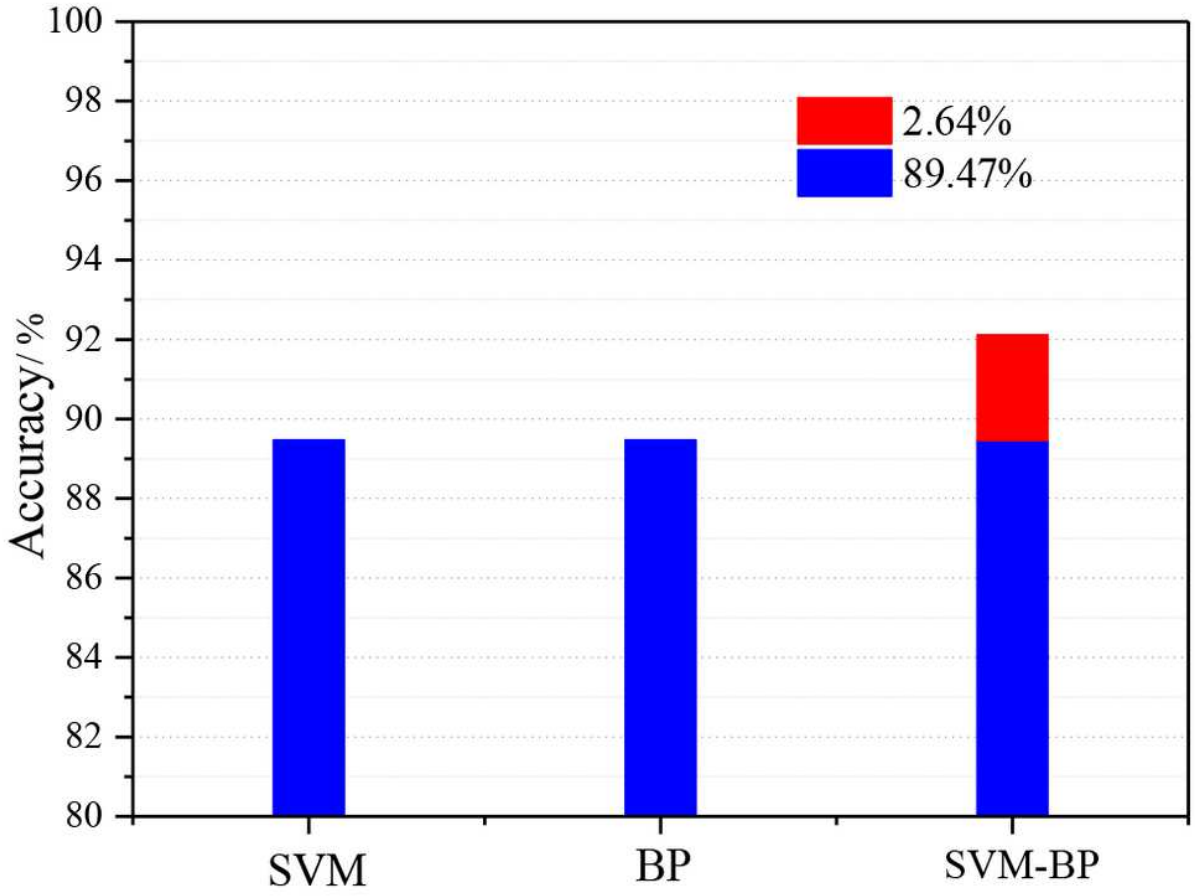

Figure 6

Comparison of the classification results of three classifiers

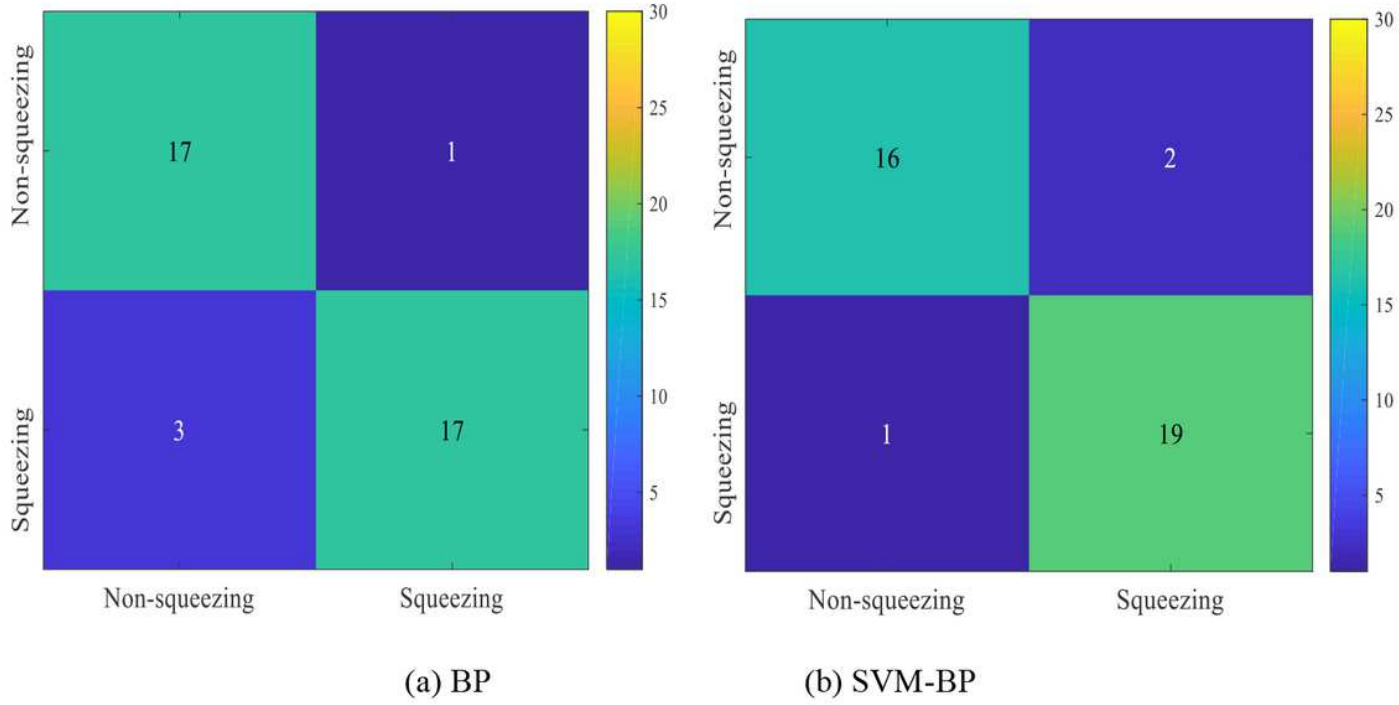

Figure 7

Confusion matrices for the BP and SVM-BP models

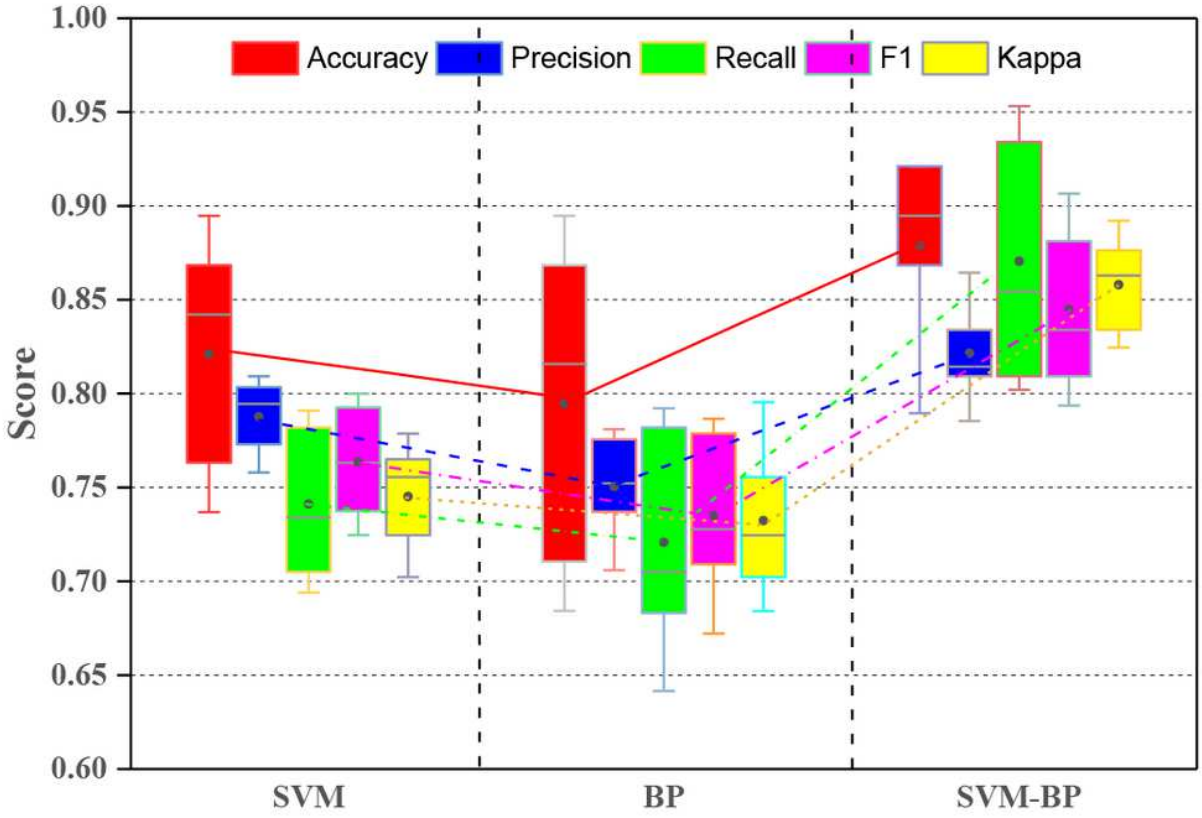

Figure 8

Comparison of the prediction performance indexes of three classifiers

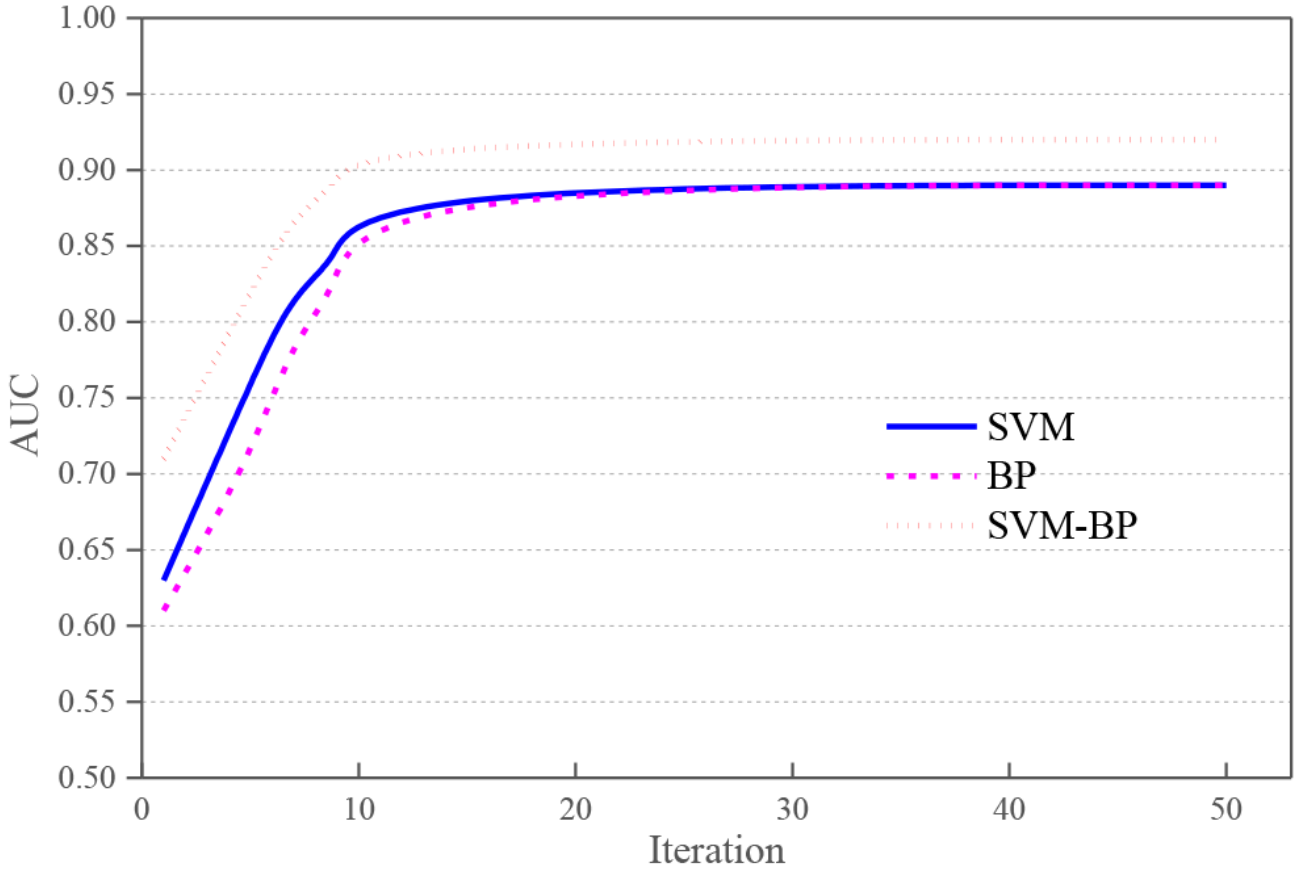

Figure 9

Comparison of the AUC values of three classifiers

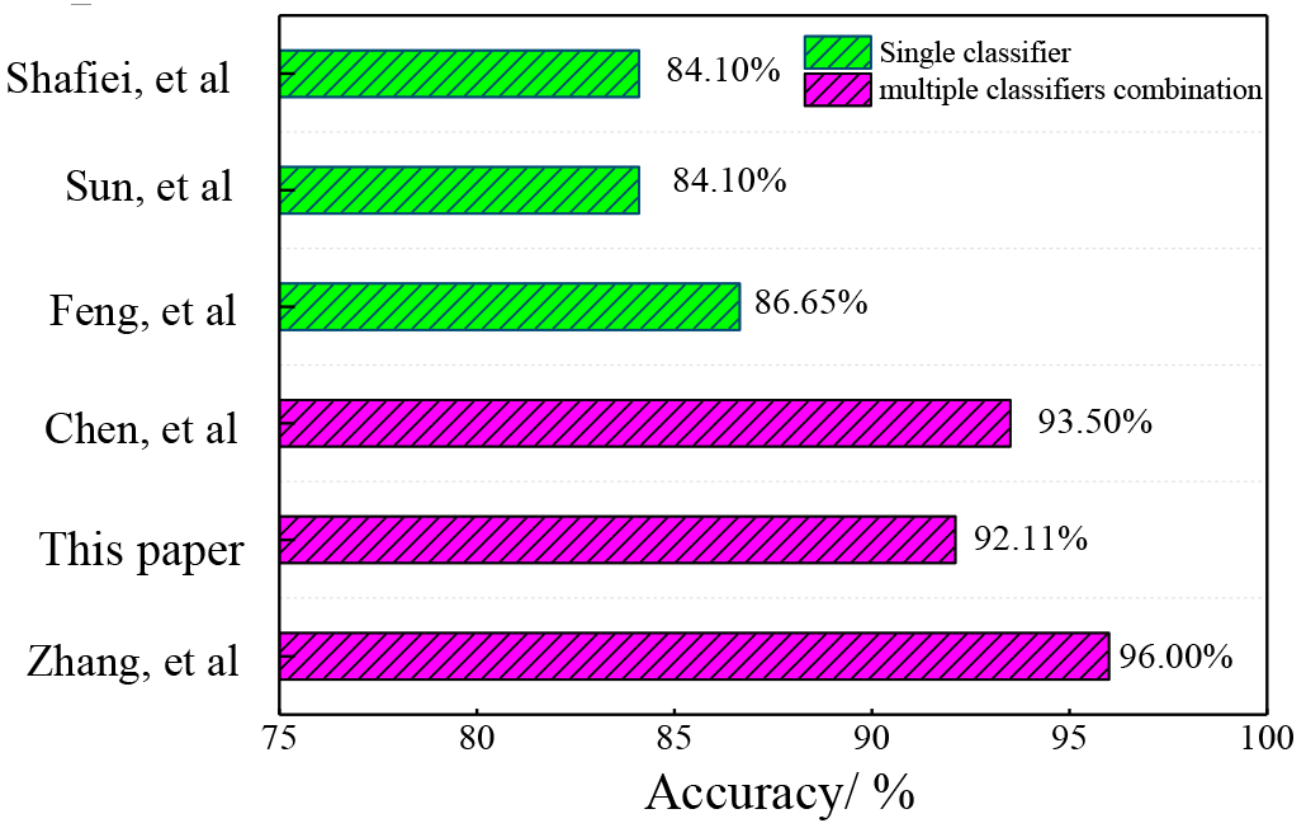

Figure 10

Comparison of classification accuracy between the proposed method and methods proposed in previous studies

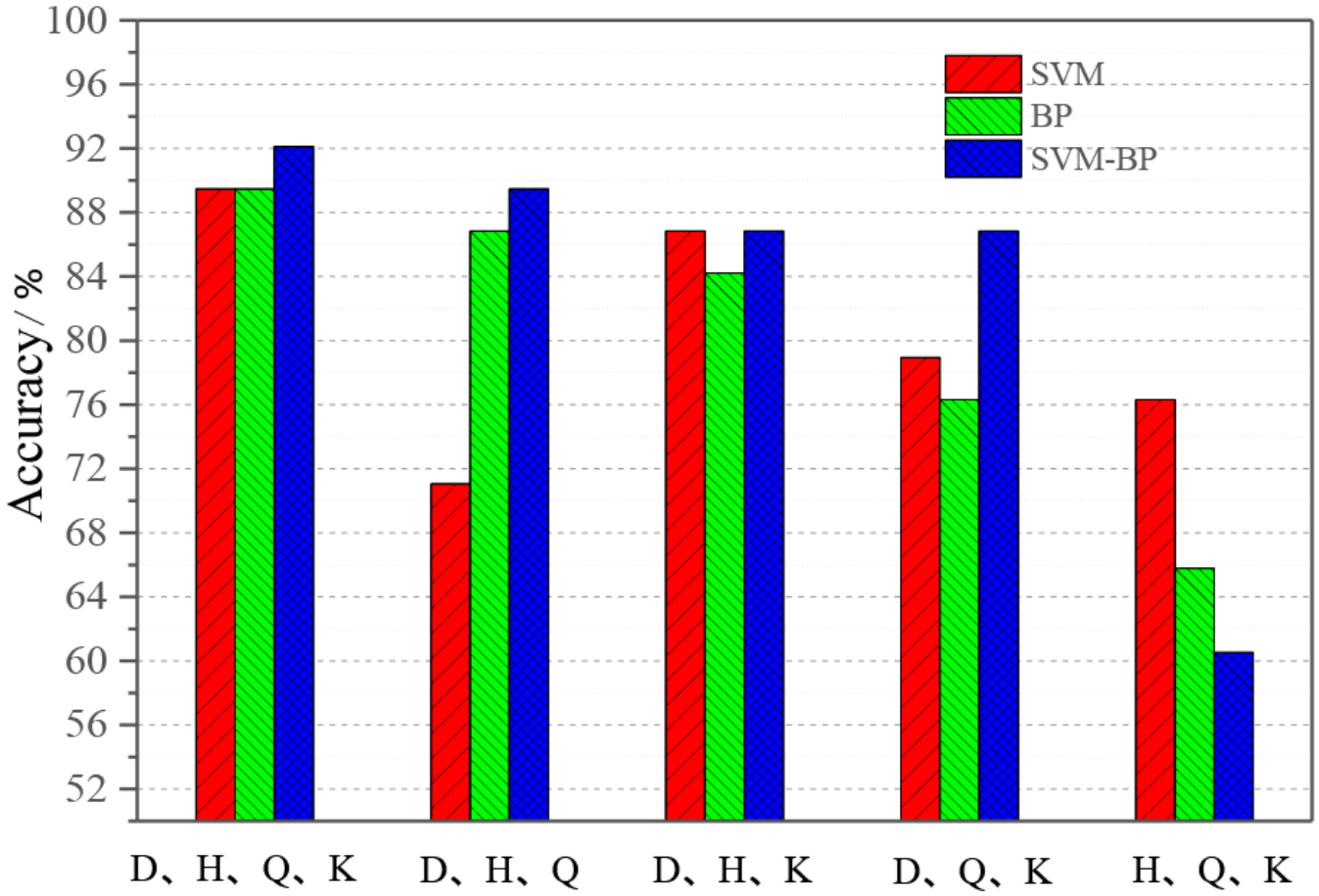

Figure 11

Comparison of the classification accuracy of the three classifiers

Supplementary Files

This is a list of supplementary files associated with this preprint. Click to download.

- Appendix.doc